

# Rapid Multi-Wavelength Optical Assessment of Circulating Blood Volume Without a Priori Data

Ekaterina V. LOGINOVA<sup>1</sup>, Tatyana V. ZHIDKOVA<sup>1</sup>,  
Mikhail A. PROSKURNIN<sup>1,2\*</sup>, and Vladimir P. ZHAROV<sup>3</sup>

<sup>1</sup>*M.V. Lomonosov Moscow State University, Chemistry Department, Moscow, 119991, Russia*

<sup>2</sup>*Agilent Technologies Partner Laboratory / M.V. Lomonosov Moscow State University, Analytical Center, Moscow, 119991, Russia*

<sup>3</sup>*Philips Classic Laser Laboratories, University of Arkansas for Medical Sciences, Little Rock, Arkansas, 72205, USA*

\*Corresponding author: Mikhail A. PROSKURNIN      E-mail: Proskurnin@gmail.com

**Abstract:** The measurement of circulating blood volume (CBV) is crucial in various medical conditions including surgery, iatrogenic problems, rapid fluid administration, transfusion of red blood cells, or trauma with extensive blood loss including battlefield injuries and other emergencies. Currently, available commercial techniques are invasive and time-consuming for trauma situations. Recently, we have proposed high-speed multi-wavelength photoacoustic/photothermal (PA/PT) flow cytometry for *in vivo* CBV assessment with multiple dyes as PA contrast agents (labels). As the first step, we have characterized the capability of this technique to monitor the clearance of three dyes (indocyanine green, methylene blue, and trypan blue) in an animal model. However, there are strong demands on improvements in PA/PT flow cytometry. As additional verification of our proof-of-concept of this technique, we performed optical photometric CBV measurements *in vitro*. Three label dyes—methylene blue, crystal violet and, partially, brilliant green—were selected for simultaneous photometric determination of the components of their two-dye mixtures in the circulating blood *in vitro* without any extra data (like hemoglobin absorption) known a priori. The tests of single dyes and their mixtures in a flow system simulating a blood transfusion system showed a negligible difference between the sensitivities of the determination of these dyes under batch and flow conditions. For individual dyes, the limits of detection of  $3 \times 10^{-6} \text{ M} - 3 \times 10^{-6} \text{ M}$  in blood were achieved, which provided their continuous determination at a level of  $10^{-5} \text{ M}$  for the CBV assessment without a priori data on the matrix. The CBV assessment with errors no higher than 4% were obtained, and the possibility to apply the developed procedure for optical photometric (flow cytometry) with laser sources was shown.

**Keywords:** Circulating blood volume assessment, spectrophotometry, methylene blue, crystal violet

---

Citation: Ekaterina V. LOGINOVA, Tatyana V. ZHIDKOVA, Mikhail A. PROSKURNIN, and Vladimir P. ZHAROV, "Rapid Multi-Wavelength Optical Assessment of Circulating Blood Volume Without a Priori Data," *Photonic Sensors*, 2016, 6(1): 42–57.

---

## 1. Introduction

Accurate and rapid assessment of circulating blood volume (CBV) is required in many clinical

applications like evaluation of outpatients and inpatients experiencing extensive blood loss [1], rapid fluid administration, and transfusion of packed

---

Received: 10 June 2015 / Revised: 2 October 2015

© The Author(s) 2015. This article is published with open access at Springerlink.com

DOI: 10.1007/s13320-015-0267-7

Article type: Regular

red blood cells (RBC) [2]; estimation of haemodilution during surgery requiring cardiopulmonary bypass without blood transfusion [3, 4]; monitoring total blood loss during surgery or blood filtration during, e.g. haemodialysis [5]; ascertainment of RBC mass at baseline preoperatively and changing in response to erythropoietic therapies [6–9], and estimation of the requirements of cardiac-assist devices [10]. However, existing techniques and assays require some improvements. Limitations include inaccuracies, high labour requirements, and slow cycle times for initial and repeat measurements.

The mostly used methods for CBV assessment use optical photometric [11–15], fluorescence [16, 17], or isotopic [18, 19] monitoring of dilution curves for contrast labels (dyes, tags, or markers) injected into an unknown blood volume. In photometric CBV assessment, a label dye (the most widespread is Evans blue [11]) is injected into a bloodstream and attaches itself to albumin [12] or in plasma [13, 14] or serum [20] with predetermined haematocrit (Ht) value [15]. The dye concentration in the bloodstream diminishes due to dilution in the whole blood volume. Its average concentration is measured with an optical photometer as a change in the absorbance at a certain wavelength. Assays using fluorescence-labeled albumins or radio-iodinated serum albumins are based on the above-mentioned label-dilution principle, but the dilution curve is measured as a fluorescence signal [16] or  $^{131}\text{I}$  pre-tagged to albumin [21, 22]. These assays cannot be used for a rapid CBV assessment without a priori data on haemoglobin (Hb) concentration and are insensitive. Isotopic dilution methods are also not reproducible [12, 23]. Tagged transfusion methods like  $^{51}\text{Cr}$  tagging of RBCs require a donor blood infusion [19]. In current practice, most clinicians agree that the transfusion of donor blood should be avoided unless necessary, thus making tagged transfusion methods less practical. Nowadays, clinical CBV assessment is implemented as *in vivo*

pulse dye densitometry (PDD) [3, 4, 24–28]. This method is based on the principles of pulse oximetry and label-dilution techniques at the absorption maximum of indocyanine green (ICG) dye [24, 29–33]. PDD provides a rapid (every 20 min–30 min, after the ICG from the previous injection is safely cleared by the liver [5]), semi-non-invasive, and convenient bedside CBV assessment [28, 34, 35] and is used for diagnostics [3, 4, 36–39] and treatment of blood losses [30, 40, 41]. PDD correlates well with  $^{131}\text{I}$  or  $^{51}\text{Cr}$  [5, 42, 43] and satisfactorily with other methods [3, 4]. The haemoglobin concentration is measured from a pre-sampled blood before an ICG injection to establish the baseline absorbance for the current patient, otherwise PDD accuracy is degraded significantly. PDD also experiences several clinical problems: (1) it is barely suitable in many liver diseases and low cardiac outputs [38, 44]; (2) signal amplitudes of optical detection are low [3]; (3) the impact of PDD on the mortality and morbidity of the critically ill patients is still under verification [28].

Thus, existing assays provide a clinical justification and examples of CBV assessment; however, no single method is feasible and reliable enough to be widely applied. Label dilution using radioisotopes or dyes is unsuitable for clinical applications, as they do not allow for frequent repeated measurements and require high concentrations of labeled proteins or contrast agents. The state-of-the-art method is PDD, and the use of ICG holds promise as the least invasive technique for measurement. However, the sensitivity and precision are not sufficient, and a priori data on Hb concentration for each patient from an independent method are required.

We have proposed high-speed multi-wavelength photoacoustic/photothermal (PA/PT) flow cytometry (PAFC/PTFC) [45–47] for *in vivo* CBV assessment with multiple dyes as PA and PT contrast labels [48]. PA and PT techniques are based on direct

measurements of absorbed energy through its non-radiative transformation into thermal effects [49–55]. Thermal changes in optical and acoustic properties of a sample upon the absorption of laser radiation allows detecting absorbances of  $10^{-10}$  abs –  $10^{-6}$  abs. units, concentrations of  $10^{-11}$  M [56] and to analyze volumes of  $10^{-12}$  L with as low as several absorbing molecules, including biotissues and nanoparticles [50, 51, 54, 57–63]. We have characterized the capability of PAFC/PTFC to monitor the clearance of several dyes (ICG, methylene blue, and trypan blue) in an animal model *in vivo* and in real time [48]. Strong dynamic PA signal fluctuations were observed, which were associated with interactions of the dyes with circulating blood cells and plasma proteins [48]. PAFC demonstrated enumeration of circulating red and white blood cells labeled with ICG and methylene blue, respectively, and the detection of rare dead cells uptaking trypan blue directly in a bloodstream [48]. PAFC/PTFC offer advanced alternatives to PDD and other CBV assays as they provide much higher sensitivity of direct measurements of absorbed energy compared with light attenuation (as in absorption spectroscopy) or re-emitted light (fluorescent techniques) [49, 64–68]. The PA technique with natural chromophores (Hb or melanin) or lowly toxic nanoparticles as PA contrast agents is currently the fastest-growing area of biomedical imaging, providing higher sensitivity and resolution at a single-cell level in deeper tissues (up to 3 cm – 5 cm) compared with other optical modalities [50, 51, 55, 63, 64]. These techniques offer the highest absorption sensitivity (100-fold – 1000-fold better than PDD/absorption spectroscopy), which allows for noninvasive detection of unlabeled biomolecules at a threshold comparable with that of fluorescence labeling (which is toxic for humans) [54, 69]. Methods are safe; the short-term temperature rise of less than or equal to  $0.01$  °C –  $1$  °C at low laser fluences ( $5$  mJ/cm<sup>2</sup> –  $20$  mJ/cm<sup>2</sup>) is

well within the laser safety standard of  $35$  mJ/cm<sup>2</sup> –  $100$  mJ/cm<sup>2</sup> at  $650$  nm –  $1100$  nm [55, 70]. The tremendous clinical potential and safety of PA/PT *in vivo* have been demonstrated in many clinical trials of other applications [64]. Examples include imaging of breast tumours at centimetre-scale depths [61, 62] or blood microvessels [55], continuous monitoring of blood oxygenation in 15-mm-diameter jugular veins despite light scattering in a 15-mm – 20-mm-thick layer of overlying tissue [71], and measurement of blood [Hb] [58]. PT determination of various Hb species (desoxyhaemoglobin, oxyhaemoglobin, carboxyhaemoglobin, methaemoglobin, cyanohaemoglobin, and hemichrome) with the limits of detection of  $10^{-8}$  M was made [72]. The error of determination of desoxyhaemoglobin vs. oxyhaemoglobin and vice versa was not above 3% – 5% for the ratio of the species of 10:1 [72]. Recently, PAFC has been developed for *in vivo* detection of circulating tumour cells and bacteria targeted by nanoparticles. As a whole, rapid PA/PT tests can be implemented as the determination of several dyes introduced in the blood as the difference in their absorption spectra can be used for the determination of their dilution. However, there are still strong demands on improvements of PAFC/PTFC.

As an additional step in the verification of the PAFC/PTFC as a CBV assessment platform [48], we focused on photometric CBV assessment with several dyes *in vitro*. Several clinically relevant absorbing dyes were tested in the presence and absence of blood to select optimum dye/wavelength combination for the simultaneous determination of components of their two-dye mixtures in blood under the conditions of CBV assessment.

## 2. Experiments

### 2.1 Reagents, solvents, and solutions

The following dyes were used: methylene blue (MB, CAS no. 61-73-4), brilliant green (BG, CAS

no. 633-03-4), crystal violet (CV, CAS no. 548-62-9), indigo carmine (CAS no. 860-22-0), bromsulphalein (CAS no. 71-67-0), and Evans blue (CAS no. 314-13-6); their stock solutions of 0.10% wt. in PBS (20 mM, pH 7.4) were used throughout. Other reagents were high-purity 0.1 M KOH, conc. cp HNO<sub>3</sub>, and p.a. acetone. Water from a TW-600RU water purification system (Nomura MicroScience Co., Ltd.; Okada, Atsugi-City, Kanagawa, Japan) was used: pH 6.8; specific resistance 18.2 MΩ·cm, Fe, 2 ppt; dissolved SiO<sub>2</sub>, 3 ppb; total ion amount, <0.2 ppb; TOC, <10 ppb. Solutions were made using a Branson 1510 ultrasonic bath (USA), power 1 W (exposure times 10 min – 15 min). The glassware was washed with acetone followed by conc. nitric acid. The blood of rats stabilized with heparin was used at the stages of blood batch and flow tests.

## 2.2 Flow manifold for *in vitro* measurements

The flow manifold (Fig. 1) consists of a circular flow system pumped with a Watson–Marlow 501U peristaltic pump (UK), a cylindrical flow cell ( $l = 15$  mm;  $16$  cm<sup>3</sup>), and a changeable (volume-adjusting) vessel (volume, 0.25 L to 6 L). All the tubing parts are from a KDM blood-transfusion system (KD Medical GmbH, Germany; length 90 cm, i.d. 0.3 cm). The system is filled with doubly distilled water, PBS, or stabilized rat blood. The dye is injected through a valve before the measurement cell to emulate the injection of the target dye in *in vivo* tests. The flow rate is kept at  $(35 \pm 1)$  mL/min (linear velocity 2 cm/s). After each measurement, the working liquid is drained to waste and washed with distilled water through a secondary injection valve (Fig. 1).

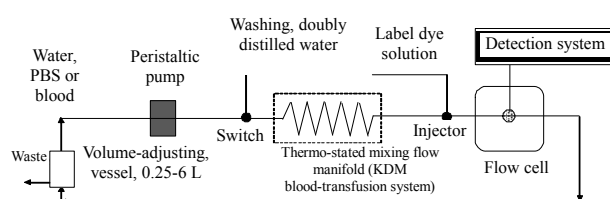


Fig. 1 Flow manifold for circulating blood volume estimation using flow photometry.

## 2.3 Measurements

A laser-based setup on the basis of a previously described continuous-wave (CW) mode PT-lens spectrometer was used [73]. The schematic (Fig. 2) was based on recording an induced refractive-index heterogeneity (thermal-lens effect, excitation: (IDL55 diode lasers, Polyus, Moscow; wavelengths 532 nm, 610 nm, 635 nm, 660 nm, and 690 nm; waist diameter,  $59.8 \mu\text{m} \pm 0.5 \mu\text{m}$ ; power range 1 mW – 20 mW) causing defocusing of a collinear probe beam (diode laser, wavelength, 808 nm; waist diameter,  $25.0 \mu\text{m} \pm 0.2 \mu\text{m}$ ; (attenuated) power, 1 mW) and, hence, a reduction in the probe beam intensity at its center by a far-field photodiode (sample-to-detector distance 180 cm) supplied with a stained-glass broadband-range (610 nm – 640 nm) bandpass filter and a 2-mm-diameter pinhole (Fig. 2).

The synchronization of the measurements was implemented by in-house written software. The PT spectrometer has a linear dynamic range of the signal of four orders of magnitude (the range of absorption coefficients for 10 mm optical pathways is  $1 \times 10^{-6} \text{ cm}^{-1}$  to  $2 \times 10^{-2} \text{ cm}^{-1}$ ) and the response time of 0.005 s – 2 s (depending on the selected measurement parameters, namely, on the data throughput rate and time, the number of points to be averaged, etc.). The spectrometer implements a secondary channel (for gathering the scattering signal, if present). The probe beam was reflected by a dichroic mirror; the residual excitation beam was removed with a stained-glass bandpass filter and after a 2-mm pinhole appeared at the primary PT detector. If the photometric or PT channel was not needed, the corresponding detector was switched off.

Spectrophotometric measurements in a batch and flow modes were made using an Agilent Cary 60 spectrophotometer (USA) with  $l=1$  mm,  $0.3$  cm<sup>3</sup>. The pH values were measured by an inoLab pH Level 1 pH-meter (Germany) with a glass pH-selective electrode (precision  $\pm 5\%$ ). Solutions were mixed with a Biosan MMS 3000 automixer and a micro-stirrer.

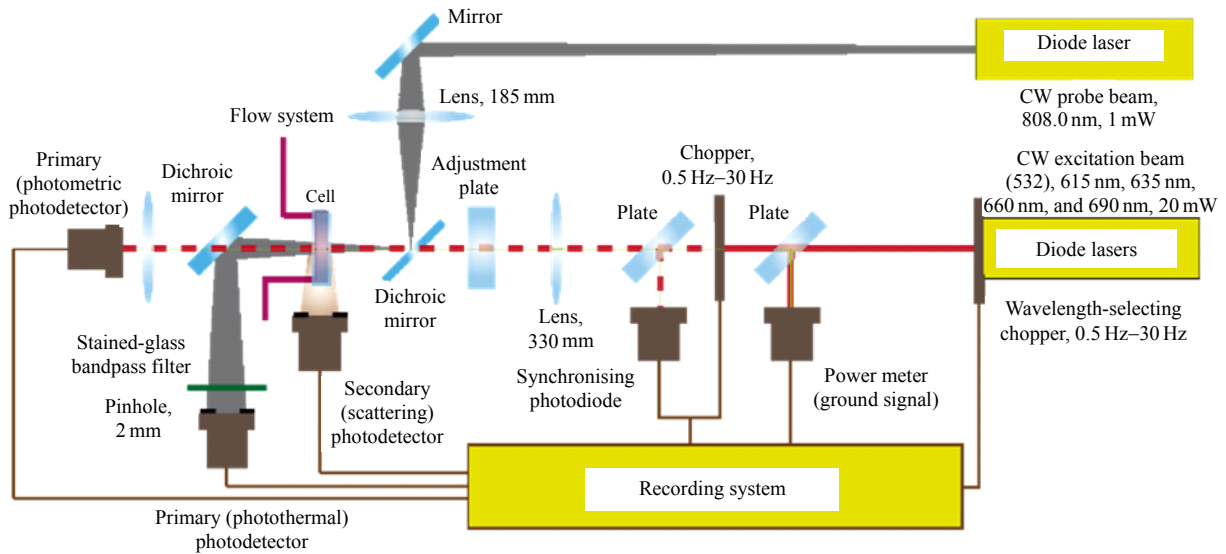


Fig. 2 Schematics of the dual-beam flow photometer / thermal-lens spectrometer.

## 2.4 CBV assessment

We used dyes for intravenous administration for optical absorbance determination of single dyes or components of two-dye mixtures in circulating blood. CBV was measured as an average of two signals for each dye to decrease the interference of both dyes on one another and thus to improve the accuracy (and determined after their dilution in circulation). The concentration of each dye diminished due to dilution. From a curve of the relative decrease in the concentration, CBV was calculated from the ratio of concentrations of the initial dye solution and the solution of dye in the blood according to the following [2, 5, 15, 74]:

$$CBV = V_0 A_0 / A_x = V_0 c_0 / c_x \quad (1)$$

where  $A$  is absorbance,  $V_0$  and  $c_0$  are initial volume and concentration of the dye solution, and  $c_x$  is the dye concentration in the blood after its dilution (Fig. 3). The determination of two components  $a$  and  $b$  of a dual-component mixture was made using two methods (1) a standard Vierordt's method at two wavelengths  $\lambda_1$  and  $\lambda_2$  [48, 75, 76]:

$$\begin{cases} A^{\lambda_1} = l(c_a \varepsilon_a^{\lambda_1} + c_b \varepsilon_b^{\lambda_1}) \\ A^{\lambda_2} = l(c_a \varepsilon_a^{\lambda_2} + c_b \varepsilon_b^{\lambda_2}) \end{cases} \quad (2)$$

and (2) using an overdetermined Vierordt's system

at four wavelengths to decrease the overall error [48]:

$$\begin{cases} \Delta A_a = A^{\lambda_1} - A^{\lambda_2} = l[c_a(\varepsilon_a^{\lambda_1} - \varepsilon_a^{\lambda_2}) + c_b(\varepsilon_b^{\lambda_1} - \varepsilon_b^{\lambda_2})] \\ \Delta A_b = A^{\lambda_3} - A^{\lambda_4} = l[c_a(\varepsilon_a^{\lambda_3} - \varepsilon_a^{\lambda_4}) + c_b(\varepsilon_b^{\lambda_3} - \varepsilon_b^{\lambda_4})] \end{cases} \quad (3)$$

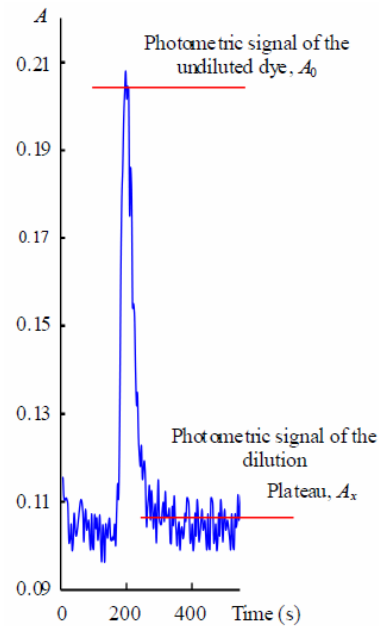


Fig. 3 Dilution curve of a dye (methylene blue) in CBV measurements.

Here,  $A$  is absorbance acquired from spectrophotometric measurements. Maxima  $\varepsilon_a^{\lambda_1} / \varepsilon_b^{\lambda_1} \times \sqrt{\varepsilon_a^{\lambda_1} \varepsilon_b^{\lambda_1}} = f(\lambda)$  and

$\varepsilon_b^{\lambda_1} / \varepsilon_a^{\lambda_1} \times \sqrt{\varepsilon_a^{\lambda_2} \varepsilon_b^{\lambda_2}} = f(\lambda)$  were used as the wavelengths for Vierordt's method. For the overdetermined Vierordt's system, (3),  $\lambda_1$  and  $\lambda_3$  are at the maxima, and  $\lambda_2$  and  $\lambda_4$  are at the minima of the absorption spectra of *a* and *b* components. The calculations of dye concentration were made taking into account the condition  $c_a/c_b = \text{const}$ , which is correct for preliminarily prepared two-dye mixtures injected into a flow [48].

## 2.5 Procedures

### 2.5.1 Tests of the flow manifold

For each dye, the solutions with a concentration of 0.01% wt – 0.1% wt. were prepared, and the solution volume varied as 250.0 mL, 500.0 mL, 1000.0 mL, 2000.0 mL, 4000.0 mL, or 6000.0 mL. The solutions were placed in a vessel connected to the flow manifold and the photometric signals were measured at a flow rate of 35 mL/min (velocity, 2 cm/s). Next, aliquots (20 mL) were probed and measured at batch conditions. Standard deviation and RSD for the same concentration and the same dye were measured for batch and flow conditions.

### 2.5.2 Spectrophotometric determination of label dyes in the flow

The 250-mL vessel of the flow manifold was filled with distilled water, which started to circulate continuously through the manifold and the flow cell. After zeroing the absorbance, an aliquot (0.2 mL) of the working solution of the dye was injected and the absorbance was continuously measured, at the working wavelength (663 nm, 624 nm, and 590 nm for MB, BG, and CV, respectively) until the constant value was attained. Next, another aliquot was injected into the same solution. The manifold was washed with 0.5 L of distilled water after measurements.

### 2.5.3 Differential photometric determination of label dyes in the flow

The 250-mL vessel of the flow manifold was

filled with a solution of the dye with absorbance of  $A=1.0-2.0$  (2.00 mL – 3.50 mL of the stock solution was diluted to 250 mL) at the working wavelength (663 nm, 624 nm, and 590 nm for MB, BG, and CV, respectively). Next, the actions were similar to Procedure 2.5.2.

### 2.5.4 Absorption spectra of label dyes in blood

Dye solutions in blood were prepared in photometric cells: 0.02 mL of the stock solution of the dye and 0.40 mL of blood were placed in a cell and mixed with a micro-stirrer followed by the determination of absorption spectra.

### 2.5.5 *In vitro* determination of label dyes under batch conditions

Stock solutions of selected dyes in blood (0.40 mL of the stock solution of the corresponding dye and 0.60 mL of blood) were used. This freshly prepared stock solution was diluted in the photometric cells alike in Procedure 2.5.4 by adding a 0.01 mL – 0.05 mL of this solution to 0.40 mL of blood. The calibrations were made at wavelengths 615 nm, 630 nm, 663 nm, and 690 nm, and the limits of detection and other performance parameters were calculated.

### 2.5.6 *In vitro* assessment of circulating blood volume

The main glass vessel of the manifold was filled with the precisely measured blood volume, and the blood started circulating through the manifold. When the regular flow through the cell was established, the zero absorbance was calibrated. Next, 0.4 mL of an aliquot of stock solutions of MB and CV or their mixture was injected, and the absorbances at 615 nm, 630 nm, 663 nm, and 690 nm were recorded until constant absorbance values were reached. The concentrations of both labels were determined from (3).

### 2.5.7 Photometric assessment of circulating blood volume in a model system

The main glass vessel of the manifold (Fig. 1)

was filled with the precisely measured blood volume, and the blood started circulating through the manifold. When the regular flow through the cell was established, the zero absorbance was calibrated. Next, 0.4 mL of a mixture of stock solutions of MB and CV was injected, and the absorbances at 615 nm, 630 nm, 663 nm, and 690 nm were recorded until constant absorbance values were reached. The concentrations of both labels were determined from (3).

### 3. Results and discussion

#### 3.1 Initial label dye tests

Multiple absorbing dyes including MB, BG, CV, congo red, indigo carmine, Evans blue, and bromsulphalein (most previously tested on humans) [25, 77–82] were tested in the presence and absence of blood to select the optimal clinically relevant dye and the wavelength combination with minimal overlapping spectral effects, low concentration (i.e. minimum toxicity), and required accuracy.

As the aim was to develop a system for rapid analysis with trace labels, we excluded indigo carmine, bromsulphalein, and Evans blue as the sensitivity of their spectrophotometric determination was low and CBV assessment would require their high concentrations. Also we excluded ICG and trypan blue, which were previously successfully tested with PAFC to expand the usable label selection [48].

The absorption spectra of the remaining labels show rather significant absorbance over blood background (Fig. 4) and do not change in the pH range 6.0–8.0 characteristic to blood.

Spectrophotometric determination of MB, CV, and BG in aqueous solutions (Procedure 2.5.2) results in limits of detection of  $1 \times 10^{-7}$  M. Differential determination of these label dyes against backgrounds of 0.5–2.0 absorbance units showed a decrease in the sensitivity by an order, which can be considered satisfactory (Table 1).

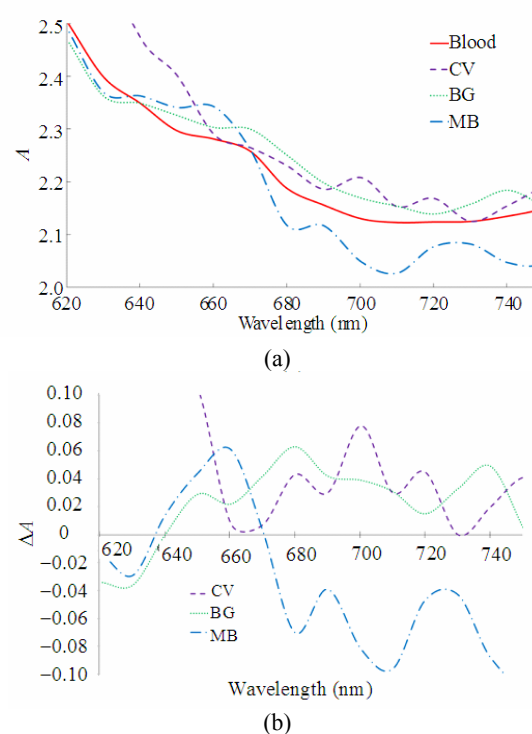


Fig. 4 Absorption spectra of blood and selected dyes in blood (a) absolute and (b) differential; crystal violet (CV,  $1.2 \times 10^{-4}$  M), Brilliant Green (BG,  $9.8 \times 10^{-5}$  M), and methylene blue (MB,  $1.3 \times 10^{-4}$  M);  $l = 1$  cm.

Table 1 Differential spectrophotometric determination of contrast dyes, pH 7.5,  $n = 5$ , and  $P = 0.95$ .

Dye ( $\lambda_{\max}$ )	$A_{\text{bkg}}$	$c_{\min}$ ( $\times 10^{-7}$ M)	Lin. calib. range ( $\times 10^6$ M)	$r$
MB (663 nm)	0.78	1	1–19	0.9961
	0.90	1	4–25	0.9933
	1.25	1	5–36	0.9721
	1.44	2	7–60	0.9687
	1.91	2	20–150	0.9383
BG (624 nm)	2.17	20	50–500	0.9561
	0.54	1	1–25	0.9965
	0.73	1	1–28	0.9886
	1.04	1	6–42	0.9819
	1.33	2	5–50	0.9696
CV (590 nm)	1.71	10	30–200	0.9042
	1.88	20	40–500	0.8826
	0.75	1	4–28	0.9716
	1.07	1	7–38	0.9667
	1.43	2	7–77	0.9511
	1.66	3	10–120	0.8922
	1.91	10	20–160	0.9677
	1.98	10	20–230	0.9637

As absorbance spectra of any dual mixtures of selected dyes overlap, Vierordt's method should be used for data treatment. The comparison of variants of Vierordt's methods showed that the best results were obtained when the ratio of molar concentrations for both labels was constant during all the tests.

According to our previous findings, a two-wavelength Vierordt's system provided the error of 20% for micromolar concentrations of both dyes in a two-dye mixture; however, the use of a four-wavelength overdetermined system decreases the error to 7% [48].

The results for the selected dyes (Tables 2, 3, and 4) confirmed this: a two-wavelength system resulted in 6% – 15% of errors in the determination of the concentration and, as a result, CBV provided a significant increase in the precision (replicability). In this case, the limits of detection of all the three dyes differ insignificantly from single dye solutions. The flow spectrophotometric determination of individual labels in the transfusion manifold (Procedure 2.5.3) showed negligible difference from the batch conditions.

Table 2 Comparison of results of determination of components of two-dye mixtures of MB and BG at pH 7.5,  $n=3$ , and  $P=0.95$ . [ $c_{add}$  is added concentration,  $c_{calc}$  is a concentration found from (3) (concentrations in  $\mu\text{M}$ )].

$c_{add}$	$c_{calc}$	
	663+690+624+550 (nm)	663 + 624 (nm)
MB		
4.3	4.4 ± 0.4 (3.6%)	4.4 ± 0.3 (3.8%)
6.4	6.3 ± 0.5 (5.5%)	6.2 ± 0.4 (2.7%)
8.6	8.8 ± 0.4 (3.0%)	8.8 ± 0.3 (2.5%)
11	10 ± 1 (5.8%)	10 ± 1 (6.1%)
13	12 ± 1 (5.0%)	12 ± 1 (5.0%)
BG		
3.3	3.5 ± 0.3 (5.0%)	3.4 ± 0.4 (3.3%)
5.0	5.2 ± 0.2 (3.6%)	5.2 ± 0.3 (3.6%)
6.6	6.6 ± 0.1 (0.1%)	6.7 ± 0.2 (0.6%)
8.3	8.3 ± 0.3 (2.6%)	8.1 ± 0.3 (2.2%)
10	9.3 ± 0.4 (6.2%)	9.5 ± 0.5 (4.8%)

Table 3 Comparison of results of determination of components of two-dye mixtures of MB and CV at pH 7.5,  $n=3$ , and  $P=0.95$ . [ $c_{add}$  is added concentration,  $c_{calc}$  is a concentration found from (3) (concentrations in  $\mu\text{M}$ )].

$c_{add}$	$c_{calc}$	
	663+690+630+590 (nm)	663+590 (nm)
MB		
4.3	4.6 ± 0.3 (6.3%)	4.1 ± 0.3 (4.1%)
6.4	6.3 ± 0.4 (2.1%)	4.2 ± 0.2 (2.7%)
8.6	8.9 ± 0.4 (3.5%)	8.1 ± 0.4 (6.0%)
11	10 ± 1 (2.0%)	10 ± 1 (9.1%)
13	12 ± 1 (4.1%)	12 ± 1 (6.4%)
CV		
3.9	4.2 ± 0.3 (7.0%)	4.5 ± 0.3 (15.2%)
5.9	6.2 ± 0.3 (6.3%)	6.3 ± 0.3 (6.8%)
7.8	6.6 ± 0.3 (4.3%)	8.8 ± 0.7 (12.6%)
10	9.8 ± 0.4 (0.3%)	10 ± 1 (6.8%)
12	12 ± 1 (1.5%)	12 ± 1 (5.0%)

For two-dye mixtures, the relative standard deviation of the determination is below 10% and is 2% – 5% for micromolar dye concentrations while using four-wavelength determination with an overdetermined Vierordt's system of equations.

The model flow manifold emulated a transfusion system: a 0.3 cm i.d, and the flow rate of 35 mL/min; the flow cell had the same diameter. The changes in the circulating blood volume within the range 250 mL – 6000 mL (Procedure 2.5.1) showed that the absorbance levels, the reproducibility, and accuracy of measurements for haemoglobin and all the dyes did not depend on the volume. CV and MB showed negligible absorption on the materials of the transfusion system, while BG was intensively absorbed by the manifold.

Table 4 Comparison of results of determination of components of two-dye mixtures of CV and BG at pH 7.5,  $n=3$ , and  $P=0.95$ . [ $c_{add}$  is added concentration,  $c_{calc}$  is a concentration found from (3) (concentrations in  $\mu\text{M}$ )].

$c_{add}$	$c_{calc}$	
	630+590+624+550 (nm)	624+590 (nm)
BG		
3.3	3.4 ± 0.3 (2.4%)	4.0 ± 0.6 (19.9%)
5.0	5.0 ± 0.1 (0.1%)	5.6 ± 0.5 (12.8%)
6.6	6.6 ± 0.1 (0.04%)	7.8 ± 0.4 (16.9%)
8.3	8.2 ± 0.2 (1.7%)	8.8 ± 0.3 (6.8%)
10	10.0 ± 0.3 (0.02%)	10 ± 1 (5.2%)
CV		
3.9	4.1 ± 0.3 (4.7%)	3.4 ± 0.3 (12.8%)
5.9	5.8 ± 0.4 (2.2%)	5.1 ± 0.6 (12.7%)
7.8	8.0 ± 0.2 (2.3%)	6.6 ± 0.5 (15.9%)
10	10 ± 1 (2.2%)	8.2 ± 0.4 (15.9%)
12	11 ± 1 (4.7%)	10 ± 1 (13.6%)

### 3.2 Assessment of dyes in blood

Brilliant green shows a very indistinct spectrum in the target wavelength range (600 nm – 650 nm) in blood, while MB and CV show very good differential spectra in 630 nm – 680 nm and 610 nm – 690 nm, respectively (Procedure 2.5.4). No correlation with their concentrations over 690 nm is due to haemoglobin absorption. The limits of detection of dyes in blood (Procedure 2.5.5) are  $3 \times 10^{-6}$  M –  $8 \times 10^{-6}$  M (Table 5); the error of determination is low, providing assessing both dyes in blood with relative standard deviations below 5% at  $10^{-5}$  M.



Table 5 Performance parameters for the assessment of contrast dyes in blood,  $n=5$  and  $P=0.95$ .

Dye	$\lambda$ (nm)	$c_{\min}$ ( $\times 10^6$ M)	Lin.cal. range ( $\times 10^3$ M)	$r$
MB	690	20	4-20	0.7830
	680	10		0.9381
	663	10		0.9694
	630	10		0.9822
	630 + 690	10		0.9896
	630 + 680	10		0.9786
	630 + 663	10		0.9268
	663 + 690	20		0.7435
	663 + 680	40		0.7648
CV	630	5	3-20	0.9934
	615	3		0.9569
	615 + 690	2		0.9766
	615 + 663	2		0.9726
	630 + 690	3		0.9897
	630 + 663	3		0.9857

Varying the wavelengths of Vierordt's system, we selected the optimum wavelengths for the overdetermined system, 630 nm and 690 nm for MB and 615 nm and 663 nm for CV (Procedure 2.5.5). For blood volumes 0.3 L – 6 L, the error of assessment was below 4%.

The optimum wavelengths fit the wavelengths of serial diode lasers, which can be used in compact detection schematics for photometric CBV assessment. We tested such a system with commercial diode lasers with 610 nm, 635 nm, 660 nm, and 690 nm. The error of measurements increased to 10%, which can be considered a satisfactory result.

### 3.3 Laser-based measurements of dyes in blood

The above values were confirmed using the developed laser-based flow spectrometer tested *in vitro* in batch and flow conditions using the available flow module as a simple model for a blood vessel and an absorption spectroscopy unit to real-time measure of absorption spectra of dye alone and in mixtures.

The setup (Fig. 2) was built using the previously optimized schematics taking into account the precision of measurements and the linear range of the thermal lens signal. The main idea is to combine photometric and PA/PT measurements in a single setup. This idea was supported by our previous data

on the use of the thermal-lens spectrometer as a single-wavelength photometer providing enough measurement precision [73]. The probe wavelength of 808 nm (marked grey in Fig. 2) was selected as it provided the minimum light absorption of the blood components and selected dyes and low scattering. The excitation beam was made of four beams of diode lasers with the same beam parameters and the wavelengths of 610 nm, 635 nm, 660 nm, and 690 nm. In a more advanced mode, the diode laser with the same beam parameters and the wavelength of 532 nm was added. The lasers were chopped in sequence synchronized with the main light chopper at a frequency of  $\psi$ , thus, every excitation on-off cycle of the thermal lens corresponded to the certain wavelength, and the frequency of the excitation with the same wavelength was  $\psi/4$  (or  $\psi/5$  for a five-wavelength mode).

In order to get the maximum information for a flowing sample (at a flow rate of 35 mL/min), high chopper frequencies are preferable, while the sensitivity of PT measurements decrease with the chopper frequency [83]. Thus, a compromise frequency of 10 Hz was used, which corresponded to 2.5 Hz frequency for a single wavelength. This corresponded to the measurement of ca. 0.15 mL of the flowing sample with a certain wavelength and 0.45 mL with other wavelengths, in cycles.

To implement dual-mode measurements, we used a dichroic mirror to separate the probe beam from the excitation. The whole excitation beam after the cell penetrated the dichroic mirror and was gathered with a focusing lens by the primary photometric detector, which was compared with pre-calibrated power meter used as the absorbance ground signal. The selection of the optimum parameters of PT measurements were discussed previously [73, 84].

The results obtained using laser-based photometry at the selected wavelengths were in good agreement with the performance parameters in

Table 5. The estimations of CBV in the test manifold similarly to Procedure 2.5.1 showed the error of assessment is below 5% for blood volumes 0.3 L – 5 L and above concentrations of dyes diminished compared with photometric measurements. The error of measurements agrees well with our previous data on PAFC measurements of CBV [48].

#### 4. Conclusions

As an additional verification of our proof-of-concept of the PAFC [48, 68, 85–90] for CBV assessment, we performed optical photometric CBV measurements *in vitro* with a specially designed multi-wavelength photothermal-lens spectrometer and a procedure for photometric determination of two dyes (methylene blue and crystal violet) in a blood-transfusion system. The precision of measurements is somewhat worse than in PDD [3, 24, 25], but better than photometric measurements [13–15, 20] and does not require any a priori data on the test system and is simple and inexpensive. Tests of single dyes and their mixtures in a flow system simulating a blood transfusion system showed micromolar limits of detection in blood with low errors. These data complements our previous findings for *in vivo* PAFC [48].

Moreover, one can see a decrease in the error of measurements by a factor of 3 – 4 compared with existing CBV techniques due to the independent determination of two dyes instead of one at two different wavelengths. The measurement provides a decrease in the contrast agent concentrations by a factor of at least 30 due to the high absorption sensitivity of PA/PT spectroscopy and low influence of scattering effects [91]. Moreover, we expect a decrease in the error of measurements by a factor of 3 – 4 compared with existing CBV techniques due to the independent determination of two dyes instead of one at two different wavelengths [48]. The determination of Hb [72] simultaneously with dye dilution will provide lower measurement time (2–4

fold) compared with photometric CBV techniques and PDD [73]. If the determination of selected dyes against high blood backgrounds ( $1 \text{ cm}^{-1} - 10 \text{ cm}^{-1}$ ) [55] shows a decrease in the sensitivity by more than an order of magnitude compared with the buffer solution, the differential PT schematics can be used in the future, which previously showed a significant accuracy (3% vs. 5% under the same conditions) and sensitivity (2 orders compared with non-differential schematics) [92, 93]. When necessary, we can increase the number of dyes to 3 or 4 in the mixture to additionally improve the accuracy of CBV measurements.

It is possible to compare the sensitivities of photometric and PT measurements for the same detector and the same laser used for measuring absorption and PT excitation. The minimum detectable linear absorption coefficients for PT and photometric (PM) measurements were calculated according to the equations previously deduced from the theory of these two methods for the conditions of shot noise determining the measurement precision [94]

$$\alpha_{\min}^{\text{PT}} = \sqrt{\frac{2h\nu_p}{\eta P_p} \Delta f} \frac{B_\infty \omega_0^2 \psi}{4P_e E_0 D_T l} \quad (4)$$

$$\alpha_{\min}^{\text{PM}} = \sqrt{\frac{h\nu_e}{\eta P_e} \Delta f} \frac{1}{l} \quad (5)$$

where  $h$  is the Planck constant,  $\nu_e$  and  $\nu_p$  are frequencies of the excitation and probe beams;  $\eta$  is the detector quantum yield;  $\Delta f$  is the detection channel bandwidth;  $\omega_0$  is the excitation beam radius;  $\psi$  is the chopper frequency in PT measurements;  $P_e$  and  $P_p$  are the excitation and probe powers,  $D_T$  is the thermal diffusivity,  $\omega_{0e}$  is the excitation beam waist radius, and  $B_\infty$  is the steady-state geometry constant of the setup optical scheme. The factor  $E_0$  is the enhancement factor of PT measurements for unit excitation laser power

$$E_0 = (-dn/dT)/\lambda_p k \quad (6)$$

where  $k$  is the thermal conductivity. The comparison of sensitivities for the same detector type [ $\eta$  and  $\Delta f$  parameters in (4) and (5)] and the same source of absorption/PT excitation is given by the equation

$$\frac{\alpha_{\min}^{\text{PT}}}{\alpha_{\min}^{\text{PM}}} = \sqrt{\frac{2\lambda_e}{\lambda_p P_p}} \frac{B_\infty \omega_0^2 \psi}{4E_0 D_T} \frac{1}{\sqrt{P_e}}. \quad (7)$$

This shows that an increase in the sensitivity depends on the geometry parameters of the setup and the parameters of the medium, in which the thermal lens is bloomed. For the experimental conditions discussed above the calculation shows that the minimum detectable linear absorption coefficient is about 250-fold lower than for photometry. This means that the significant diminishing of dye doses to get reliable PT signals compared with current clinical doses (for PDD, 2.5 mg/mL – 5 mg/mL) can be made when shifting from optical photometric to PT measurements of CBV.

We anticipate that this non-invasive rapid real-time CBV assessment is valuable for monitoring surgical patients in the operating room, especially those undergoing surgery with predictable substantial blood loss. The high capacity of a multi-wavelength PTFC technique would provide CBV assessment with expected advantages compared with existing assays. Successful completion of these specific aims will provide a novel method for CBV measurements *in vivo* and will shift clinical paradigms by achieving high sensitivity (50-fold – 100-fold higher than that using existing techniques), rapid turnaround (a few minutes vs. hours due to exclusion of any a priori information on the patient), and high accuracy (4% – 7% vs. 15% – 30%). The proposed platform can be further applied to PA or PAFC measurements of multiple blood parameters including a total Hb amount, Ht, oxygenation, abnormal blood cells (e.g., sickle), and Hb composition e.g., meta-, carboxy-, nitroso- or HbS (e.g., in sickle cells) during various

diseases like anaemia as well as on use of encapsulated dyes (e.g. ICG). This system can be also used along with optical-fiber sensors [95]. After proof-of-concept on a small animal model, we will plan a preclinical validation with a larger animal model (e.g., sheep), eventually clinical validation, and feasibility testing (e.g., evaluation of measurement sites including finger, nose, lip, ear, and hand veins).

## Acknowledgment

The work is supported by the Russian Science Foundation, grant no. 14-23-00012. We are grateful to Agilent Technologies – Russia and its CEO, Dr. Konstantin Evdokimov, for Agilent equipment used in this study.

**Open Access** This article is distributed under the terms of the Creative Commons Attribution 4.0 International License (<http://creativecommons.org/licenses/by/4.0/>), which permits unrestricted use, distribution, and reproduction in any medium, provided you give appropriate credit to the original author(s) and the source, provide a link to the Creative Commons license, and indicate if changes were made.

## References

- [1] A. Lozhkin, T. Makedonskaya, G. Pakhomova, and O. Loran, “Estimation of the trauma severity degree in injured with associated injuries depending on the blood loss,” *Vox Sanguinis*, 2010, 99(Suppl 1): 435–436.
- [2] D. M. Jr. Takanishi, E. N. Biuk-Aghai, M. Yu, F. Lurie, H. Yamauchi, H. C. Ho, *et al.*, “The availability of circulating blood volume values alters fluid management in critically ill surgical patients,” *American Journal of Surgery*, 2009, 197(2): 232–237.
- [3] W. Baulig, E. O. Bernhard, D. Bettex, D. Schmidlin, and E. R. Schmid, “Cardiac output measurement by pulse dye densitometry in cardiac surgery,” *Anaesthesia*, 2005, 60(10): 968–973.
- [4] M. Kroon, A. B. Groeneveld, and Y. M. Smulders, “Cardiac output measurement by pulse dye densitometry: comparison with pulmonary artery thermodilution in post-cardiac surgery patients,” *Journal of Clinical Monitoring and Computing*, 2005, 19(6): 395–399.

- [5] S. Henschen, M. W. Busse, S. Zisowsky, and B. Panning, "Determination of plasma volume and total blood volume using indocyanine green: a short review," *Journal of Medicine*, 1993, 24(1): 10–27.
- [6] L. Donner and V. Maly, "Total blood volume in some blood diseases. II. results in pernicious anemia, anemia following hemorrhage, polycythemia vera, secondary polyglobulia and leukemia," *Sbornik Lekarsky*, 1955, 57(5): 125–136.
- [7] L. K. Vricella, J. M. Louis, E. Chien, and B. M. Mercer, "Blood volume determination in obese and normal-weight gravidas: the hydroxyethyl starch method," *American Journal of Obstetrics and Gynecology*, 2015, 213(3): 408.e1–408.e6.
- [8] A. Joffe, N. Khandelwal, M. Hallman, and M. Treggiari, "Assessment of circulating blood volume with fluid administration targeting euvolemia or hypervolemia," *Neurocritical Care*, 2015, 22(1): 82–88.
- [9] D. Konno, R. Nishino, Y. Ejima, E. Ohnishi, K. Sato, and S. Kurosawa, "Assessment of the perioperative factors contributing to the hemodynamic changes during surgery in ten patients with pheochromocytoma," *Masui. Japanese Journal of Anesthesiology*, 2013, 62(4): 421–425.
- [10] K. Tanaka, T. Sato, C. Kondo, I. Yada, H. Yuasa, M. Kusagawa, *et al.*, "Hematological problems during the use of cardiac assist devices: clinical experiences in Japan," *Artificial Organs*, 1992, 16(2): 182–188.
- [11] N. M. Keith, L. G. Rowntree, and J. T. Geraghty, "A method for the determination of plasma and blood volume," *Archives of Internal Medicine*, 1915, 16(4): 547–557.
- [12] W. Jegier, J. Maclaurin, W. Blankenship, and J. Lind, "Comparative study of blood volume estimation in the newborn infant using I-131 labeled human serum albumin (Ihsa) and T-1824," *Scandinavian Journal of Clinical and Laboratory Investigation*, 1964, 16: 125–132.
- [13] N. N. Uglova, A. I. Volozhin, and V. E. Potkin, "Method for determination of the circulating blood volume with Evans blue T-1824," *Patologicheskaiia Fiziologiia i Eksperimentalnaia Terapiia*, 1972, 16(2): 80–82.
- [14] S. A. Glants and V. V. Shevchuk, "A micromethod for the determination of blood volume in laboratory animals," *Laboratornoe Delo*, 1963, 16: 49.
- [15] O. A. Kovalev and V. N. Grishanov, "Determination of the volume of circulating blood by using Evans blue dye," *Laboratornoe Delo*, 1976, 11: 664–667.
- [16] C. M. Gillen, A. Takamata, G. W. Mack, and E. R. Nadel, "Measurement of plasma volume in rats with use of fluorescent-labeled albumin molecules," *Journal of Applied Physiology*, 1994, 76(1): 485–489.
- [17] G. R. Tudhope and G. M. Wilson, "A comparison of 86Rb, 32P and 51Cr as labels for red blood cells," *Journal of Physiology*, 1955, 128(3): 61–62.
- [18] T. P. Sivachenko, V. K. Kalina, V. P. Ishchenko, A. K. Belous, and V. I. Kapustnik, "Repeated semi-automatic determination of circulating blood volume," *Vrachebnoe Delo*, 1977, (7): 25–28.
- [19] S. J. Gray and K. Sterling, "Determination of circulating red cell volume by radioactive chromium," *Science*, 1950, 112(2902): 179–180.
- [20] B. M. Datsenko, N. I. Pilipenko, V. I. Gubskii, and R. A. Sherlanov, "The determination of the volume of circulating plasma using the indicator T-1824," *Laboratornoe Delo*, 1990, 11: 32–34.
- [21] J. G. Gibson, A. M. Seligman, W. C. Peacock, J. C. Aub, J. Fine, and R. D. Evans, "The distribution of red cells and plasma in large and minute vessels of the normal dog, determined by radioactive isotopes of iron and iodine," *Journal of Clinical Investigation*, 1946, 25(6): 848–857.
- [22] V. K. Modestov and A. T. Tsygankov, "Thyroid function tests using triiodothyronine labeled with I-131," *Meditinskaiia Radiologiia*, 1965, 10: 11–13.
- [23] I. A. Frid, V. I. Stoliarov, A. I. Evtiukhin, and M. I. Bernshtein, "Hemodynamic indices and the volume of circulating blood in the surgical treatment of cancer of the esophagus and cardiac portion of the stomach," *Vestnik Khirurgii Imeni I. I. Grekova*, 1976, 117(10): 92–96.
- [24] M. Haruna, K. Kumon, N. Yahagi, Y. Watanabe, Y. Ishida, N. Kobayashi, and T. Aoyagi, "Blood volume measurement at the bedside using ICG pulse spectrophotometry," *Anesthesiology*, 1998, 89(6): 1322–1328.
- [25] T. Imai, K. Takahashi, H. Fukura, and Y. Morishita, "Measurement of cardiac output by pulse dye densitometry using indocyanine green: a comparison with the thermodilution method," *Anesthesiology*, 1997, 87(4): 816–822.
- [26] J. A. Tichy, M. Loucka, Z. M. Trefny, M. Hojerova, J. Svacinka, J. Muller, *et al.*, "New clearance evaluation method for hepatological diagnostics," *Physiological Research*, 2009, 58(2): 287–292.
- [27] C. K. Hofer, M. T. Ganter, and A. Zollinger, "What technique should I use to measure cardiac output?," *Current Opinion in Critical Care*, 2007, 13(3): 308–317.
- [28] R. W. Goy, J. W. Chiu, and C. C. Loo, "Pulse dye densitometry: a novel bedside monitor of circulating

- blood volume,” *Annals of the Academy of Medicine, Singapore*, 2001, 30(2): 192–198.
- [29] H. Sugimoto, O. Okochi, M. Hirota, N. Kanazumi, S. Nomoto, S. Inoue, *et al.*, “Early detection of liver failure after hepatectomy by indocyanine green elimination rate measured by pulse dye-densitometry,” *Journal of Hepato-Biliary-Pancreatic Surgery*, 2006, 13(6): 543–548.
- [30] R. G. Hoff, G. W. van Dijk, A. Algra, C. J. Kalkman, and G. J. Rinkel, “Fluid balance and blood volume measurement after aneurysmal subarachnoid hemorrhage,” *Neurocritical Care*, 2008, 8(3): 391–397.
- [31] K. Sha, M. Shimokawa, M. Morii, K. Kikumoto, S. Inoue, K. Kishi, *et al.*, “Optimal dose of indocyanine-green injected from the peripheral vein in cardiac output measurement by pulse dye-densitometry,” *Masui. Japanese Journal of Anesthesiology*, 2000, 49(2): 172–176.
- [32] N. Taguchi, S. Nakagawa, K. Miyasaka, M. Fuse, and T. Aoyagi, “Cardiac output measurement by pulse dye densitometry using three wavelengths,” *Pediatric Critical Care Medicine*, 2004, 5(4): 343–350.
- [33] Y. Fujita, T. Yamamoto, M. Fuse, N. Kobayashi, S. Takeda, and T. Aoyagi, “Pulse dye densitometry using indigo carmine is useful for cardiac output measurement, but not for circulating blood volume measurement,” *European Journal of Anaesthesiology*, 2004, 21(8): 632–637.
- [34] T. Imai, C. Mitaka, T. Nosaka, A. Koike, S. Ohki, Y. Isa, *et al.*, “Accuracy and repeatability of blood volume measurement by pulse dye densitometry compared to the conventional method using <sup>51</sup>Cr-labeled red blood cells,” *Intensive Care Medicine*, 2000, 26(9): 1343–1349.
- [35] T. Kunihara, Y. Wakamatsu, A. Adachi, M. Koyama, N. Shiiya, S. Sasaki, *et al.*, “Clinical evaluation of hepatic blood flow and oxygen metabolism during thoracoabdominal aortic surgery using pulse dye-densitometry combined with hepatic venous oxygen saturation,” *Kyobu Geka. Japanese Journal of Thoracic Surgery*, 2000, 53(7): 551–557.
- [36] T. Hori, S. Yagi, T. Iida, K. Taniguchi, K. Yamagiwa, C. Yamamoto, *et al.*, “Stability of cirrhotic systemic hemodynamics ensures sufficient splanchnic blood flow after living-donor liver transplantation in adult recipients with liver cirrhosis,” *World Journal of Gastroenterology*, 2007, 13(44): 5918–5925.
- [37] H. Akita, Y. Sasaki, T. Yamada, K. Gotoh, H. Ohigashi, H. Eguchi, *et al.*, “Real-time intraoperative assessment of residual liver functional reserve using pulse dye densitometry,” *World Journal of Surgery*, 2008, 32(12): 2668–2674.
- [38] R. E. Stauber, D. Wagner, V. Stadlbauer, S. Palma, G. Gurakuqi, D. Kniepeiss, *et al.*, “Evaluation of indocyanine green clearance and model for end-stage liver disease for estimation of short-term prognosis in decompensated cirrhosis,” *Liver International: Official Journal of the International Association for the Study of the Liver*, 2009, 29(10): 1516–1520.
- [39] T. Takazawa, K. Nishikawa, I. Watanabe, and F. Goto, “Preoperative evaluation of hemodynamics using indocyanine green clearance meter in patients with peritonitis from gastrointestinal perforation,” *Masui the Japanese Journal of Anesthesiology*, 2005, 54(3): 260–264.
- [40] R. Hoff, G. Rinkel, B. Verweij, A. Algra, and C. Kalkman, “Blood volume measurement to guide fluid therapy after aneurysmal subarachnoid hemorrhage: a prospective controlled study,” *Stroke*, 2009, 40(7): 2575–2577.
- [41] O. Okochi, T. Kaneko, H. Sugimoto, S. Inoue, S. Takeda, and A. Nakao, “ICG pulse spectrophotometry for perioperative liver function in hepatectomy,” *Journal of Surgical Research*, 2002, 103(1): 109–113.
- [42] E. C. Bradley and J. W. Barr, “Determination of blood volume using indocyanine green (cardio-green) dye,” *Life Sciences*, 1968, 7(17): 1001–1007.
- [43] H. Fukuda, M. Kawamoto, and O. Yuge, “A comparison of finger and nose probes in pulse dye-densitometry measurements of cardiac output, blood volume and mean transit time,” *Masui the Japanese Journal of Anesthesiology*, 2001, 50(12): 1351–1356.
- [44] F. Bremer, A. Schiele, and K. Tschaikowsky, “Cardiac output measurement by pulse dye densitometry: a comparison with the Fick's principle and thermodilution method,” *Intensive Care Medicine*, 2002, 28(4): 399–405.
- [45] D. A. Nedosekin, E. I. Galanzha, E. Dervishi, A. S. Biris, and V. P. Zharov, “Super-resolution nonlinear photothermal microscopy,” *Small*, 2014, 10(1): 135–142.
- [46] D. A. Nedosekin, M. Sarimollaoglu, E. I. Galanzha, R. Sawant, V. P. Torchilin, V. V. Verkhusha, *et al.*, “Synergy of photoacoustic and fluorescence flow cytometry of circulating cells with negative and positive contrasts,” *Journal of Biophotonics*, 2013, 6(5): 425–434.
- [47] Y. A. Menyayev, D. A. Nedosekin, M. Sarimollaoglu, M. A. Juratli, E. I. Galanzha, V. V. Tuchin, *et al.*,

- “Optical clearing in photoacoustic flow cytometry,” *Biomedical Optics Express*, 2013, 4(12): 3030–3041.
- [48] M. A. Proskurnin, T. V. Zhidkova, D. S. Volkov, M. Sarimollaoglu, E. I. Galanzha, D. Mock, *et al.*, “*In vivo* multispectral photoacoustic and photothermal flow cytometry with multicolor dyes: A potential for real-time assessment of circulation, dye-cell interaction, and blood volume,” *Cytometry Part A the Journal of the International Society for Analytical Cytology*, 2011, 79A(10): 834–847.
- [49] S. E. Bialkowski, *Photothermal spectroscopy methods for chemical analysis*. New York: Wiley-Interscience, 1996.
- [50] L. V. Wang, “Multiscale photoacoustic microscopy and computed tomography,” *Nature Photonics*, 2009, 3(9): 503–509.
- [51] S. Mallidi, T. Larson, J. Tam, P. P. Joshi, A. Karpouk, K. Sokolov, *et al.*, “Multiwavelength photoacoustic imaging and plasmon resonance coupling of gold nanoparticles for selective detection of cancer,” *Nano Letters*, 2009, 9(8): 2825–2831.
- [52] V. P. Zharov and V. S. Letokhov, *Laser optoacoustic spectroscopy*. Berlin-Heidelberg: Springer-Verlag, 1986.
- [53] V. P. Zharov, “Laser optoacoustic spectroscopy in chromatography,” in *Laser analytical spectrochemistry*, Boston, MA: Bristol, pp. 229–271, 1986.
- [54] M. Harada, M. Shibata, T. Kitamori, and T. Sawada, “Application of coaxial beam photothermal microscopy to the analysis of a single biological cell in water,” *Analytica Chimica Acta*, 1995, 299(3): 343–347.
- [55] L. V. Wang, *Photoacoustic imaging and spectroscopy*. New York: Taylor & Francis/CRC Press, 2009.
- [56] M. A. Proskurnin, “Photothermal spectroscopy,” in *Laser spectroscopy for sensing: fundamentals, techniques and applications*. Cambridge: Woodhead Publ Ltd, 2014, pp. 313–361.
- [57] V. P. Zharov and D. O. Lapotko, “Photothermal imaging of nanoparticles and cells,” *IEEE Journal of Selected Topics in Quantum Electronics*, 2005, 11(4): 733–751.
- [58] I. Y. Petrova, R. O. Esenaliev, Y. Y. Petrov, H. P. Brecht, C. H. Svensen, J. Olsson, *et al.*, “Optoacoustic monitoring of blood hemoglobin concentration: a pilot clinical study,” *Optics Letters*, 2005, 30(13): 1677–1679.
- [59] Y. Y. Petrov, I. Y. Petrova, I. A. Patrikeev, R. O. Esenaliev, and D. S. Prough, “Multiwavelength optoacoustic system for noninvasive monitoring of cerebral venous oxygenation: a pilot clinical test in the internal jugular vein,” *Optics Letters*, 2006, 31(12): 1827–1829.
- [60] R. G. Kolkman, W. Steenbergen, and T. G. van Leeuwen, “*In vivo* photoacoustic imaging of blood vessels with a pulsed laser diode,” *Lasers in Medical Science*, 2006, 21(3): 134–139.
- [61] S. Ermilov, A. Stein, A. Conjusteau, R. Gharieb, R. Lacewell, T. Miller, *et al.*, “2007 Detection and noninvasive diagnostics of breast cancer with 2-color laser optoacoustic imaging system,” in *Proc. SPIE*, vol. 6437, pp. 643703–643711, 2007.
- [62] S. E. Vaartjes, J. C. G. van Hespren, J. M. Klaase, *et al.*, “2007 First clinical trials of the Twente photoacoustic mammoscope (PAM),” in *Proc. SPIE*, vol. 6629, pp. 662912–662917, 2007.
- [63] D. Razansky, M. Distel, C. Vinegoni, R. Ma, N. Perrimon, R. W. Koster, *et al.*, “Multispectral opto-acoustic tomography of deep-seated fluorescent proteins *in vivo*,” *Nature Photonics*, 2009, 3(7): 412–417.
- [64] V. V. Tuchin, A. Tárnok, and V. P. Zharov, “*In vivo* flow cytometry: a horizon of opportunities,” *Cytometry Part A*, 2011, 79A(10): 737–745.
- [65] A. V. Brusnichkin, D. A. Nedosekin, E. I. Galanzha, Y. A. Vladimirov, E. F. Shevtsova, M. A. Proskurnin, *et al.*, “Ultrasensitive label-free photothermal imaging, spectral identification, and quantification of cytochrome c in mitochondria, live cells, and solutions,” *Journal of Biophotonics*, 2010, 3(12): 791–806.
- [66] E. I. Galanzha, M. S. Kokoska, E. V. Shashkov, J. W. Kim, V. V. Tuchin, and V. P. Zharov, “*In vivo* fiber-based multicolor photoacoustic detection and photothermal purging of metastasis in sentinel lymph nodes targeted by nanoparticles,” *Journal of Biophotonics*, 2009, 2(8–9): 528–539.
- [67] E. I. Galanzha, J. W. Kim, and V. P. Zharov, “Nanotechnology-based molecular photoacoustic and photothermal flow cytometry platform for *in-vivo* detection and killing of circulating cancer stem cells,” *Journal of Biophotonics*, 2009, 2(12): 725–735.
- [68] V. P. Zharov, E. I. Galanzha, E. V. Shashkov, J. W. Kim, N. G. Khlebtsov, and V. V. Tuchin, “Photoacoustic flow cytometry: principle and application for real-time detection of circulating single nanoparticles, pathogens, and contrast dyes *in vivo*,” *Journal of Biomedical Optics*, 2007, 12(5): 051503-1–051503-14.
- [69] A. D. Modestov, Y. V. Pleskov, V. P. Varnin, and I. G. Teremetskaya, “Synthetic semiconductor diamond

- electrodes: a study of electrochemical activity in a redox system solution,” *Russian Journal of Electrochemistry*, 1997, 33(1): 55–60.
- [70] E. I. Galanzha and V. P. Zharov, “*In vivo* photoacoustic and photothermal cytometry for monitoring multiple blood rheology parameters,” *Cytometry Part A*, 2011, 79A(10): 746–757.
- [71] S. A. Lozhkin, “Depth of Boolean functions in a complete basis,” *Vestnik Moskovskogo Universiteta Seriya I Matematika Mekhanika*, 1996, 51(2): 80–83.
- [72] A. Brusnichkin, D. Nedosekin, E. Ryndina, M. Proskurnin, E. Gleb, D. Lapotko, *et al.*, “Determination of various hemoglobin species with thermal-lens spectrometry,” *Moscow University Chemistry Bulletin*, 2009, 64(1): 45–54.
- [73] M. A. Proskurnin, A. G. Abroskin, and D. Y. Radushkevich, “A dual-beam thermal lens spectrometer for flow analysis,” *Journal of Analytical Chemistry*, 1999, 54(1): 91–97, 1999.
- [74] A. A. Riley, Y. Arakawa, S. Worley, B. W. Duncan, and K. Fukamachi, “Circulating blood volumes: a review of measurement techniques and a meta-analysis in children,” *ASAIO Journal*, 2010, 56(3): 260–264.
- [75] J. Karpinska, A. Sokol, and M. Rozko, “Applicability of derivative spectrophotometry, bivariate calibration algorithm, and the vierordt method for simultaneous determination of ranitidine and amoxicillin in their binary mixtures,” *Analytical Letters*, 2009, 42(8): 1203–1218.
- [76] E. Dinc and F. Onur, “Comparative study of the ratio spectra derivative spectrophotometry, derivative spectrophotometry and Vierordt's method applied to the analysis of oxfendazole and oxclozanide in a veterinary formulation,” *Analisis*, 1997, 25(3): 55–59.
- [77] M. A. Yaseen, J. Yu, B. Jung, M. S. Wong, and B. Anvari, “Biodistribution of encapsulated indocyanine green in healthy mice,” *Molecular Pharmaceutics*, 2009, 6(5): 1321–1332.
- [78] V. Saxena, M. Sadoqi, and J. Shao, “Enhanced photo-stability, thermal-stability and aqueous-stability of indocyanine green in polymeric nanoparticulate systems,” *Journal of Photochemistry and Photobiology. B: Biology*, 2004, 74(1): 29–38.
- [79] N. M. Shestakov, “Complexity and inadequacy of current methods of determining circulating blood volume and the feasibility of a simpler and faster method of determining it,” *Terapevticheskii Arkhiv*, 1977, 49(3): 115–120.
- [80] C. Tsopelas and R. Sutton, “Why certain dyes are useful for localizing the sentinel lymph node,” *Journal of Nuclear Medicine*, 2002, 43(10): 1377–1382.
- [81] A. B. Dawson, H. M. Evans, and G. H. Whipple, “Blood volume studies: III. behavior of large series of dyes introduced into the circulating blood,” *American Journal of Physiology*, 1920, 51(2): 232–256.
- [82] K. Shoemaker, J. Rubin, G. L. Zumbro, and R. Tackett, “Evans blue and gentian violet: alternatives to methylene blue as a surgical marker dye,” *Journal of Thoracic and Cardiovascular Surgery*, 1996, 112(2): 542–544.
- [83] A. Smirnova, M. A. Proskurnin, S. N. Bendrysheva, D. A. Nedosekin, A. Hibara, and T. Kitamori, “Thermo-optical detection in microchips: From macro- to micro-scale with enhanced analytical parameters,” *Electrophoresis*, 2008, 29(13): 2741–2753.
- [84] M. A. Proskurnin and A. G. Abroskin, “Optimization of optical system parameters in dual-beam thermal lens spectrometry,” *Journal of Analytical Chemistry*, 1999, 54(5): 401–408.
- [85] D. A. Nedosekin, M. Sarimollaoglu, E. V. Shashkov, E. I. Galanzha, and V. P. Zharov, “Ultra-fast photoacoustic flow cytometry with a 0.5 MHz pulse repetition rate nanosecond laser,” *Optics Express*, 2010, 18(8): 8605–8620.
- [86] D. A. Nedosekin, E. V. Shashkov, E. I. Galanzha, L. Hennings, and V. P. Zharov, “Photothermal multispectral image cytometry for quantitative histology of nanoparticles and micrometastasis in intact, stained and selectively burned tissues,” *Cytometry A*, 2010, 77(11): 1049–1058.
- [87] E. V. Shashkov, M. Everts, E. I. Galanzha, and V. P. Zharov, “Quantum dots as multimodal photoacoustic and photothermal contrast agents,” *Nano Letters*, 2008, 8(11): 3953–3958.
- [88] V. P. Zharov, E. I. Galanzha, Y. Menyaev, and V. V. Tuchin, “*In vivo* high-speed imaging of individual cells in fast blood flow,” *Journal of Biomedical Optics*, 2006, 11(5): 054034.
- [89] V. P. Zharov, E. I. Galanzha, E. V. Shashkov, N. G. Khlebtsov, and V. V. Tuchin, “*In vivo* photoacoustic flow cytometry for monitoring of circulating single cancer cells and contrast agents,” *Optics Letters*, 2006, 31(24): 3623–3625.
- [90] V. P. Zharov, E. I. Galanzha, and V. V. Tuchin, “Photothermal flow cytometry *in vitro* for detection and imaging of individual moving cells,” *Cytometry A*, 2007, 71(4): 191–206.
- [91] S. E. Bialkowski, *Photothermal spectroscopy*

*methods for chemical analysis*. New York: A Wiley-Interscience publication, 1996.

- [92] M. A. Proskurnin and M. E. Volkov, "Mode-mismatched dual-beam differential thermal lensing with optical scheme design optimized using expert estimation for analytical measurements," *Applied Spectroscopy*, 2008, 62(4): 439–449.
- [93] S. E. Bialkowski, X. Gu, P. E. Poston, and L. S. Powers, "Pulsed-laser excited differential photothermal deflection spectroscopy," *Applied Spectroscopy*, 1992, 46(9): 1335–1345.
- [94] A. Y. Luk'yanov, G. B. Vladykin, M. A. Novikov, and Y. I. Yashin, "Comparison of the capability limits of some optical detectors for liquid chromatography," *Journal of Analytical Chemistry*, 1999, 54(7): 633–638.
- [95] P. Roriz, A. Ramos, J. Santos, and J. Simões, "Fiber optic intensity-modulated sensors: a review in biomechanics," *Photonic Sensors*, 2012, 2(4): 315–330.